# Supporting Information

## Enhanced cycling stability and rate capability of the graphene-supported commercialized Vat Blue 4 anode for advanced Li-ion batteries

Hongwei Kang,[a,b,1] Quanwei Ma,[b,c,1] Rui Wang,[b,c] Longhai Zhang,[a,b,c]* Shuisheng Chen,[a]* Xinrui Wang, [a] Chaofeng Zhang [a,b,c]*

[a] *School of Chemistry and Materials Engineering, Anhui Provincial Key Laboratory for Degradation and Monitoring of Pollution of the Environment, Fuyang Normal University, Fuyang 236037, China*

[b] *Key Laboratory of Advanced Energy Materials Chemistry (Ministry of Education), College of Chemistry, Nankai University, Tianjin 300071, China*

[c] *Institutes of Physical Science and Information Technology, Anhui University, Hefei 230601, China*

*Corresponding Authors: zlhedu@163.com (L. Zhang); chenss@fynu.edu.cn (S. Chen); cfz@ahu.edu.cn (C. Zhang)

[1] These authors contributed equally to this work

**Preparation of VB4/rGO Composite:** GO was first prepared by modified Hummers methods.[1] Subsequently, 120 mg GO and 0.3 mL ammonium hydroxide (Macklin, AR, 25%-28%) were dispersed in 60 mL DI-water under sonication for 0.5 h. Then, 400 mg VB4 (Bide Pharmatech Ltd. 99%) and 1.5 mL hydrazine hydrate (Aladdin, 98%) were added inside and kept at 100 ℃ for 1.5 h. After cooled down to room temperature, the products were obtained by vacuum filtration with water and ethyl alcohol (Hushi, 99.7%) washing. Finally, the sample was dried in a vacuum at 80 ℃.

**Preparation of rGO:** GO was first prepared by modified Hummers methods.1 Subsequently, 120 mg GO and 0.3 mL ammonium hydroxide (Macklin, AR, 25%-28%) were dispersed in 60 mL DI-water under sonication for 0.5 h. Then, 1.5 mL hydrazine hydrate (Aladdin, 98%) were added inside and kept at 100 ℃ for 1.5 h. After cooled down to room temperature, the products were obtained by vacuum filtration with water and ethyl alcohol (Hushi, 99.7%) washing. Finally, the sample was dried in a vacuum at 80 ℃ (62.4 mg, yield: 52%). According to the yield of rGO (52%, $\gamma\% = m_{rGO}/m_{GO}*100\%$), the mass of rGO in VB4/rGO can be calculated to be about 62.4 mg (*i.e.* 120*$\gamma$%). Therefore, the contents of rGO and VB4 in VB4/rGO hybrid can be calculated to be about 13% and 87% ($\omega_{rGO}\% = m_{rGO}/(m_{rGO}+m_{VB4})*100\%$), respectively.

**Materials characterizations:** The morphology of samples was observed by SEM (JEOL-6300F) and TEM (JEM-2100). The compositions and specific surface areas were conducted on X-ray photoelectron spectroscopy (XPS, ESCALAB 250Xi), Fourier-transform infrared (FT-IR, Vertex80+Hyperion2000), and BET (ASAP-2010

surface area analyzer).

**Electrochemical Measurements:** The anodes were prepared by mixing products (70 wt%), Ketjen Black (20 wt%), and polyvinylidene fluoride (PVDF, 10 wt%) in NMP solvent. The areal mass loading of VB4/rGO is approximately 0.5-1.0 mg $cm^{-2}$. Afterward, the electrodes, coin-type cells (CR2032), separator, Li foil, and electrolyte (1 M $LiPF_6$) were assembled in a glove box. The Li-ion storage performance was measured on NEWARE tester (5 V/10 mA, Shenzhen, China) and electrochemical workstation (PMC1000) at temperature of 25 ºC.

**Theoretical Calculation:** VB4 molecule adsorbed within the graphite sheets was constructed. Periodic density functional theory (DFT) computations were performed by using Material studio software. The generalized gradient approximation (GGA) and Perdew-Burke-Ernzerhof (PBE) functions were employed.[2] The plane-wave cutoff energy is 300 eV. An energy tolerance of $10^{-6}$ eV $atom^{-1}$ was used for the convergence. The charge-density differences and the density of states on this adsorbed model were explored. Additionally, the adsorption energy ($\Delta E$) was calculated as follows:

$$\Delta E = E_{\mathrm{VB4/rGO}} - E_{\mathrm{VB4}} - E_{rGO}$$

in which the $E_{\mathrm{VB4}}$, $E_{\mathrm{rGO}}$, and $E_{\mathrm{VB4/rGO}}$ are the energies of the VB4 molecule, rGO model, and the total adsorbed system, respectively.

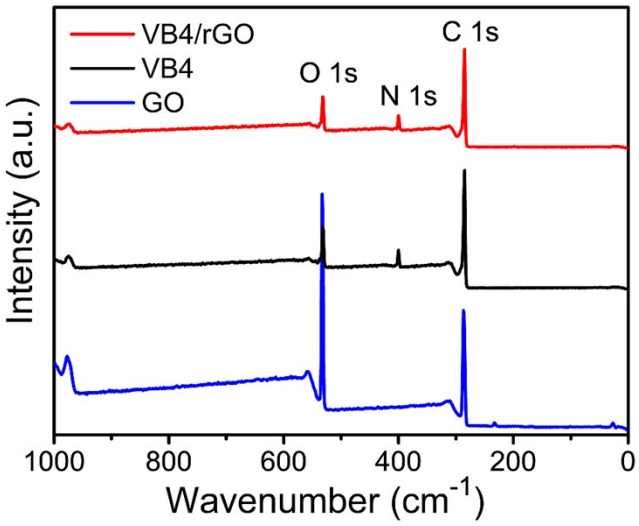


**Fig. S1** XPS survey spectra of the VB4/rGO, VB4, and GO.

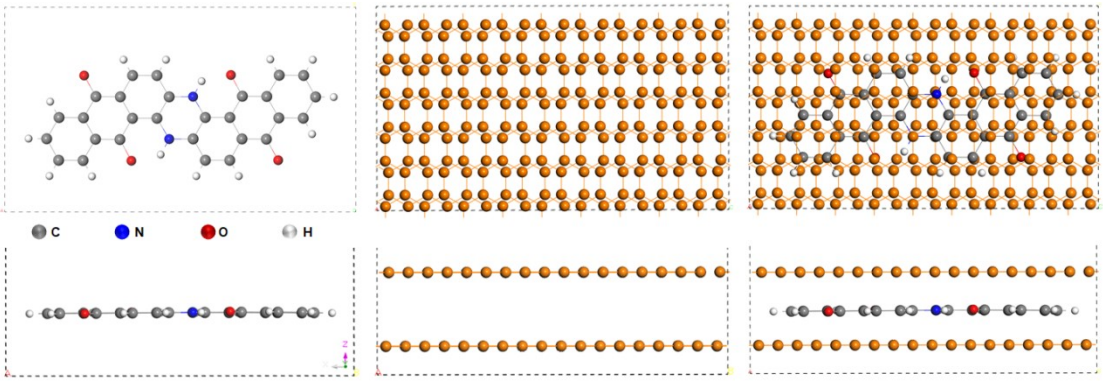


**Fig. S2** The optimized models of pristine VB4 and VB4/rGO hybrid.

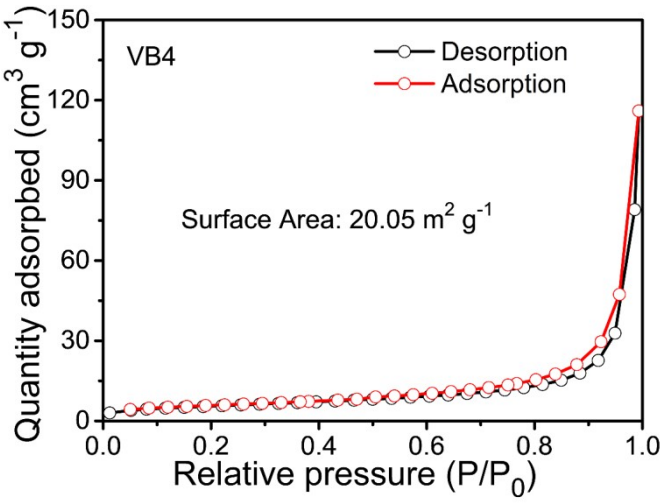


**Fig. S3** $N_2$ adsorption/desorption isotherms of the pristine VB4.

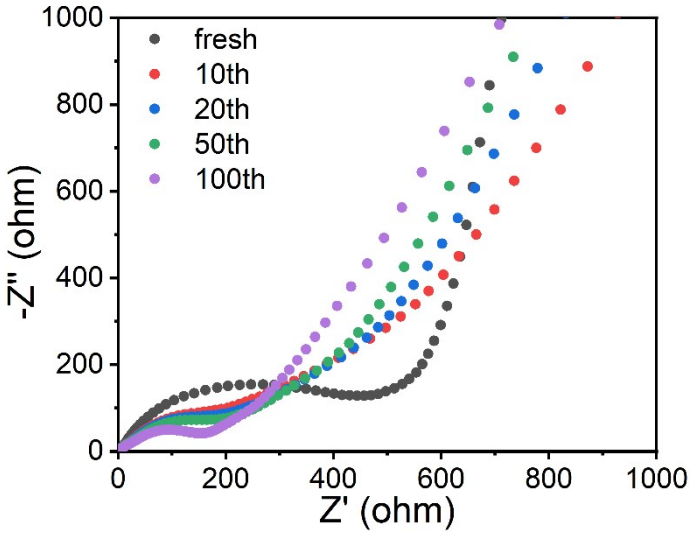


**Fig.S**4 EIS plots for VB4/rGO upon cycling at the current density of 1 A $g^{-1}$.

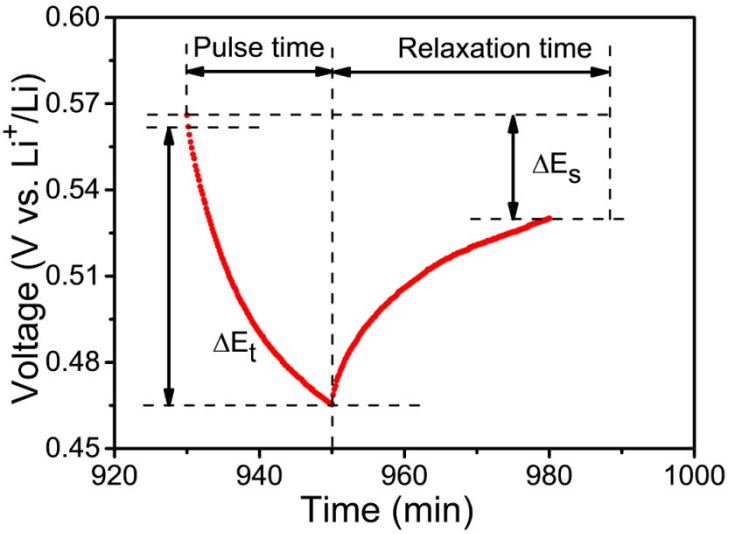


**Fig. S5** E *vs.* t profiles for the GITT measurement.

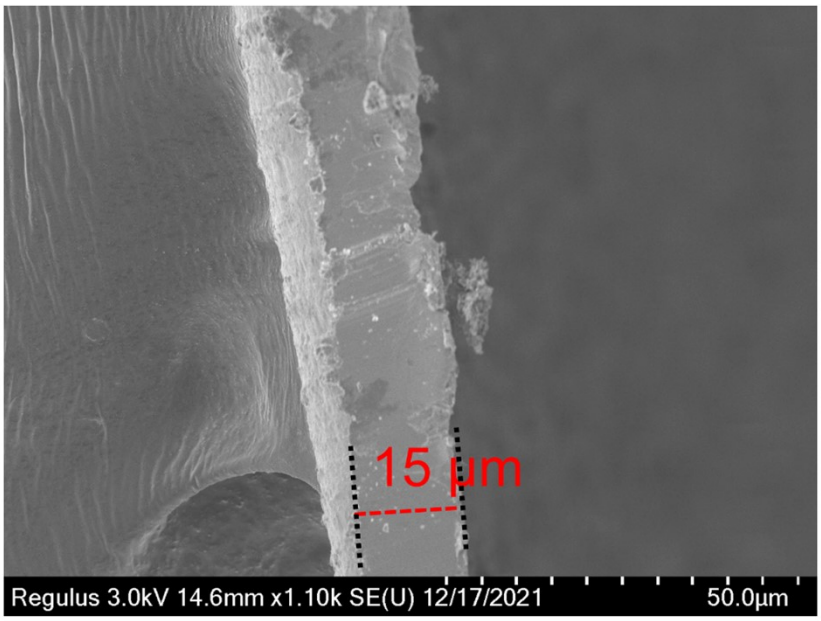


**Fig. S6** SEM cross-section image of the VB4/rGO electrode.

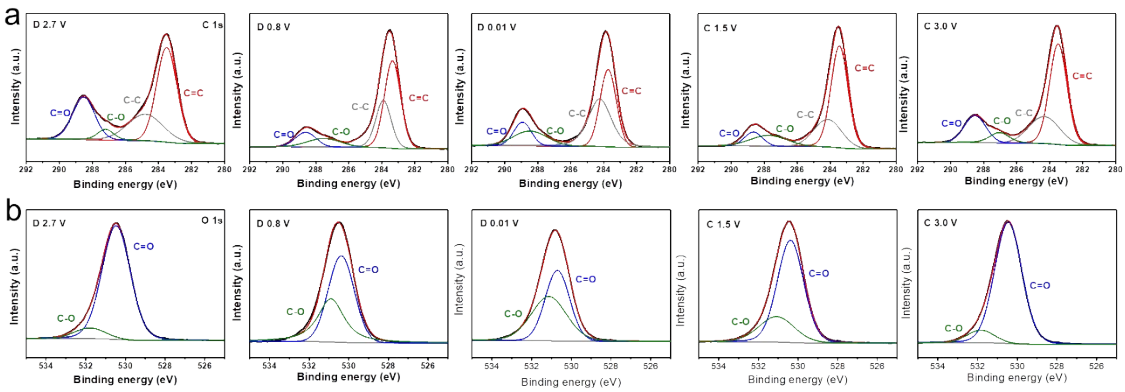


**Fig. S7** The ex-situ XPS spectra of VB4/rGO anode under different charge/discharge states: (a) C 1s and (b) O 1s.

**Table S1**. Comparison of the Li-storage performance of reported organic anode materials with resultant VB4/rGO.

| Electrode materials | electrolyte | Capacity (mAh $g^{-1}$) | Cycling performance (mAh $g^{-1}$) | Ref. |
|---|---|---|---|---|
| VB4/rGO | 1 M $LiPF_6$ | 1097@0.1 A $g^{-1}$<br>315@5.0 A $g^{-1}$ | 537@1 A $g^{-1}$,<br>1000 cycles | This work |
| HPB-COOH | 1 M $LiPF_6$ | 997@0.1 A $g^{-1}$<br>290@5.0 A $g^{-1}$ | 750@2 A $g^{-1}$<br>500 cycles | 3 |
| $Li_4C_8H_2O_6$ | 1 M $LiPF_6$ | 251.7@0.05 A $g^{-1}$<br>102.8@2.0 A $g^{-1}$ | 102.8@2.0 A $g^{-1}$<br>220 cycles | 4 |
| Tp-Ta-COF | 1 M $LiPF_6$ | 441@0.2 A $g^{-1}$<br>195@2.0 A $g^{-1}$ | 441@0.2 A $g^{-1}$<br>800 cycles | 5 |
| cPAN | 1 M $LiPF_6$ | 551@0.05 A $g^{-1}$<br>213@5.0 A $g^{-1}$ | 810@1 A $g^{-1}$<br>1090 cycles | 6 |
| TP–OH–COF | 1 M $LiPF_6$ | 764.1@0.1 A $g^{-1}$<br>114.7@10 A $g^{-1}$ | 156.3@5.0 A $g^{-1}$<br>8000 cycles | 7 |
| Cl-cHBC | 1.3 M $LiPF_6$ | 393@0.1 A $g^{-1}$<br>75@20 A $g^{-1}$ | 220@8.0 A $g^{-1}$<br>1000 cycles | 8 |
| Tp-Azo-COF | 1 M LiTFSI | 613.8@0.1 A $g^{-1}$<br>90.76@2.4 A $g^{-1}$ | 305.9@1 A $g^{-1}$<br>3000 ycles | 9 |
| $Li_6$ -HAT | 1 M LiTFSI | 588@0.1 A $g^{-1}$<br>210@1.6 A $g^{-1}$ | 294.5@0.8 A $g^{-1}$<br>3000 cycles | 10 |
| EA | 1 M $LiPF_6$ | 644@0.1 A $g^{-1}$<br>162@1 A $g^{-1}$ | 162@1 A $g^{-1}$<br>1000 cycles | 11 |
| Te-BnV | 1 M $LiPF_6$ | 502@0.1 A $g^{-1}$<br>252@2 A $g^{-1}$ | 502@0.1 A $g^{-1}$<br>40 cycles | 12 |

**Reference**


1. Y. Wu, B. Wang, Y. Ma, Y. Huang, N. Li, F. Zhang and Y. Chen, *ACS Nano*, 2008, **2**, 463-470.
2. J. Perdew, K.Burke and M. Ernzerhof, *Phys. Rev. Lett.*, 1996, **77**, 3865-3868.
3. J. Zhang, Y. Xia, C. Ye, H. Qiu, N. Zhang, G. Yin, G. Ren, C. Chen, Y. Yuan and H.-L. Wang, *Energy Storage Mater.*, 2021, **42**, 109-117.
4. H. Zhang, Y. Lin, L. Chen, D. Wang, H. Hu and C. Shen, *ChemElectroChem*, 2020, **7**, 306-313.
5. G. Zhao, Y. Sun, Y. Yang, C. Zhang, Q. An and H. Guo, *EcoMat*, 2022, e212221.
6. W. Zhang, M. Sun, J. Yin, E. Abou-Hamad, U. Schwingenschlogl, P. Costa and H. N. Alshareef, *Angew Chem Int Ed Engl*, 2021, **60**, 1355-1363.
7. L. Zhai, G. Li, X. Yang, S. Park, D. Han, L. Mi, Y. Wang, Z. Li and S. Y. Lee, *Advanced Functional Materials*, 2021, **32**, 2108798.
8. K. Eom, M. Kang, J. H. Park, S. H. Joo, J. Park, J. Lee, S. K. Kwak, S. Ahn and S. J. Kang, *Journal of Materials Chemistry A*, 2021, **9**, 20607-20614.
9. G. Zhao, Y. Zhang, Z. Gao, H. Li, S. Liu, S. Cai, X. Yang, H. Guo and X. Sun, *ACS Energy Letters*, 2020, **5**, 1022-1031.
10. S.-B. Xia, T. Liu, W.-J. Huang, H.-B. Suo, F.-X. Cheng, H. Guo and J.-J. Liu, *Journal of Energy Chemistry*, 2020, **51**, 303-311.
11. T. Xia, Y. Wang, B. Wang, Z. Yang, G. Pan, L. Zhang and J. Zhang, *ChemElectroChem*, 2019, **6**, 4765-4772.
12. G. Li, B. Zhang, J. Wang, H. Zhao, W. Ma, L. Xu, W. Zhang, K. Zhou, Y. Du and G. He, *Angew Chem Int Ed Engl*, 2019, **58**, 8468-8473.